Imprinting a Three-dimensional Skyrmion in a Bose-Einstein Condensate Via a Raman Process

Zekai Chen¹, S.X. Hu² and Nicholas P. Bigelow^{1*}

 ^{1*}Department of Physics and Astronomy, University of Rochester, Rochester, 14627, New York, USA.
 ²Laboratory for Laser Energetics, University of Rochester, Rochester, 14623, New York, USA.

*Corresponding author(s). E-mail(s): nicholas.bigelow@rochester.edu;

Abstract

We describe an experimental protocol for the creation of a three-dimensional topological defect, a skyrmion, in a pseudo-spin-1/2 Bose-Einstein condensate (BEC) confined in a spin-independent harmonic trap. We show that one can imprint the skyrmion on the BEC within a few tens of microseconds using a Raman process with the structured laser fields. We numerically solved the mean-field Gross-Pitaevskii equation to examine our imprinting scheme, and found that all parameters we use are experimentally feasible.

Keywords: 3D Skyrmion, Bose-Einstein Condensate, Raman Process

1 Introduction

Topological defects in quantum fluids, and specifically spinor superfluids, have been an important topic in quantum physics for decades. Perhaps the earliest examples involved the role of such defects in understanding the properties of superfluid ³He [1–4]. More recently, the realization of samples of ultracold atoms has offered an ideal system for studying topological defects in spinor superfluids, including defects such as vortices and skyrmions. Various methods

3D Skyrmion imprinting in a BEC

2

have been developed to create topological defects in a spinor Bose–Einstein condensate (BEC). These include applying a time dependent inhomogeneous magnetic field (i.e. a moving, structured magnetic field) to the BEC [5–10] as well as a phase imprinting scheme based on a Raman process using structured laser fields [11–18]. Among the spectrum of possible topological defects, the skyrmion – a map from a monopole on a n-sphere to the \mathbb{R}^n space – has drawn particular attention because its connections not only to superfluids, but also to liquid crystals, magnetic semiconductors and superconductors [3, 4, 19–22]. Furthermore, the ease with which atomic BECs can be of manipulated and controlled of makes the spinor BEC an ideal system in which to study the properties and dynamics of the skyrmion.

To create topological defects in a BEC, the Raman process imprinting scheme is known for its simplicity and speed. To date, however, the Raman technique has only been used to create two-dimensional topological defects such as vortices and two-dimensional skyrmions. In this work, we propose an imprinting scheme to create a three-dimensional skyrmion with spatially varying three-dimensional features that belong to the third homotopy group π_3 [24] by introducing a third far-detuned laser to the Raman interaction. The imprinting scheme is designed for a pseudo-spin-1/2 BEC trapped in a spherically symmetric harmonic potential, and the imprinting time scale is several tens of microseconds. We verified our scheme by numerically simulating the imprinting process based on mean-field Gross-Pitaevskii theory and we have found good agreement with our theoretical predictions. We then determine practical experimental parameters that could be used to realize the 3D skyrmion.

This paper is organized as follows: in section.2, we discuss the general theory of a pseudo-spin-1/2 BEC, how to map a 3D Skyrmion to the wavefunction of a pseudo-spin-1/2 BEC and imprint the topological defect onto a BEC by allowing the BEC state to time evolve under a certain Hamiltonian. In section.3 we construct the desired spatially varying effective two-level Hamiltonian via a Raman process with multiple off-resonant lasers. In section.4 we examine the effectiveness of our imprinting scheme by a mean-field Gross-Pitaevskii numerical simulation of the imprinting process. Then in section.5 we briefly discuss how to observe the topological defects created in the experiment, and we summarize and conclude the paper in section.6.

2 3D Skyrmion in a pseudo-spin-1/2 Bose-Einstein condensate

2.1 General theory of pseudo-spin-1/2 spinor Bose-Einstein condensate

Generally, for a pseudo-spin-1/2 BEC, the spinor wavefunction can be written as

$$\vec{\psi}(\vec{r},t) = \sqrt{\rho(\vec{r},t)}\vec{\zeta}(\vec{r},t)e^{i\varphi}, \tag{1}$$

where $\sqrt{\rho(\vec{r},t)}$ is the scalar part of the wavefunction with spatially varying density $\rho(\vec{r},t)$, $\vec{\zeta}(\vec{r},t) = (\zeta_1,\zeta_2)^T$ is the spinor part of the wavefunction that satisfies $|\vec{\zeta}|^2 = 1$, and $\varphi = \varphi(\vec{r},t)$ is the local U(1) gauge phase. The scalar part of the wavefunction satisfies

$$\int \rho(\vec{r}, t)d^3r = N,\tag{2}$$

where N is the number of atoms in the BEC.

Since the spinor part $\vec{\zeta}$ is normalized, we can write the spinor as

$$\vec{\zeta} = (x_1 \pm ix_2, x_3 \pm ix_4)^T, \tag{3}$$

where x_1 , x_2 , x_3 and $x_4 \in \mathbb{R}$, and they satisfy the normalization condition $|x_1|^2 + |x_2|^2 + |x_3|^2 + |x_4|^2 = 1$. Therefore, the spinor $\vec{\zeta}$ can be regarded as a vector defined on a three-dimensional sphere, S^3 , in four-dimensional Euclidean space, \mathbb{R}^4 (see for example details given in Ref.[24]). Consider a monopole vector field on S^3 , where the vectors are perpendicular to the sphere at every point. Generally, one can parameterize a point on S^3 in the spherical coordinates (λ, β, η)

$$x_{1} = \cos \lambda$$

$$x_{2} = \sin \lambda \cos \beta$$

$$x_{3} = \sin \lambda \sin \beta \cos \eta$$

$$x_{4} = \sin \lambda \sin \beta \sin \eta,$$
(4)

where $\lambda \in [0, \pi]$, $\beta \in [0, \pi]$, $\eta \in [0, 2\pi)$. If we map the monopole field on S^3 to three-dimensional Euclidean space, \mathbb{R}^3 , parameterized by (r, θ, ϕ) (stereographic projection), then the vector field in \mathbb{R}^3 forms a 3D skyrmion. To get a picture of a 3D skyrmion, one can start from the interpretation and visualization of a 2D skyrmion. By considering a monopole spin texture on a two-dimensional sphere S^2 and unwraping the sphere into a 2D Euclidean space \mathbb{R}^2 via stereographic projection the result is a 2D skyrmion spin texture on the 2D plane. Similarly, if we consider a monopole spin texture on a three-dimensional sphere S^3 , and unwrap the three-dimensional sphere into a 3D Euclidean space \mathbb{R}^3 , the resulting spin texture in \mathbb{R}^3 is a 3D skyrmion. Specifically, if we construct a map between (λ, β, η) and (r, θ, ϕ) then the three-dimensional spinor $\vec{\zeta}(\vec{r})$ will carry the 3D skyrmion spin texture (see also Ref.[23, 24]). One can tell if the system carries the 3D skyrmion by calculating the winding number (charge) [23–26],

$$Q = \frac{1}{2\pi^2} \int_{\Sigma} \sin^2 \lambda \sin \beta \left| \frac{\partial(\lambda, \beta, \eta)}{\partial(r, \theta, \phi)} \right| d^3r, \tag{5}$$

where $|\frac{\partial(\lambda,\beta,\eta)}{\partial(r,\theta,\phi)}|$ is the Jacobian between coordinates (λ,β,η) and (r,θ,ϕ) , and Σ is any closed surface enclosing the 3D skyrmion.

2.2 Imprinting a 3D skyrmion in a Bose-Einstein condensate

In section.2.1, we discussed the general theory of mapping a 3D skyrmion in \mathbb{R}^4 to a pseudo-spin-1/2 BEC wavefunction in \mathbb{R}^3 . In this section, we address the issue of how to imprint such a topological defect onto the spinor wavefunction of a BEC.

Like in the previous works on imprinting topological defects on spinor BECs [11–18], we consider using a monopole-like synthetic magnetic field to cause the spatially varying spin rotation to imprint the topological structure on the spin-1/2 BEC. Specifically, we consider a Hamiltonian of the form

$$H_e = \frac{1}{2}\hbar\alpha\vec{r}\cdot\vec{\sigma},\tag{6}$$

where α is the amplitude of the interaction, $\vec{r} = (x, y, z)^T$ and $\vec{\sigma} = (\sigma_x, \sigma_y, \sigma_z)^T$ is the vector of Pauli matrices. Such a Hamiltonian takes the same form as the Hamiltonian of a spin-1/2 system interacting with a monopole-like magnetic field. Using the Hamiltonian in eqn.(6), we can construct the time evolution operator, $U(\vec{r},t) = e^{-iH_e t/\hbar}$, with the exact form

$$U = \cos \gamma \mathbb{1} - i\vec{n} \cdot \vec{\sigma} \sin \gamma$$

$$= \begin{pmatrix} \cos \gamma - i \sin \gamma \cos \theta & -i \sin \gamma \sin \theta e^{-i\phi} \\ -i \sin \gamma \sin \theta e^{i\phi} & \cos \gamma + i \sin \gamma \cos \theta \end{pmatrix}, \tag{7}$$

where $\gamma = \gamma(r,t) = \alpha r t/2\hbar$, $\vec{n} = (\sin\theta\cos\phi, \sin\theta\sin\phi, \cos\theta)^T$ is the unit vector on S² and 1 is the identity matrix. If we apply the time evolution operator to the spinor wavefunction with initial spinor state $\vec{\zeta}_0 = (1,0)^T$, then the spinor state after evolving under H_e for a time T_0 becomes

$$\vec{\zeta}_s = \begin{pmatrix} \cos \gamma - i \sin \gamma \cos \theta \\ -i \sin \gamma \sin \theta e^{i\phi} \end{pmatrix} = U \vec{\zeta}_0. \tag{8}$$

Considering eqn.(4) and eqn.(7), if we let $\gamma = \lambda$, $\theta = \beta$ and $\phi = \eta$, then the gauge transformation U becomes the map between S^3 and \mathbb{R}^3 .

In our setup, the BEC is confined in an isotropic harmonic trap with a Thomas-Fermi radius R_0 . If we let the evolution time be $T_0 = 2\hbar\pi/\alpha R_0$, then we get $\gamma \in [0, \pi]$ if $r \in [0, R_0]$, $\theta \in [0, \pi]$ and $\phi \in [0, 2\pi)$, and $\vec{\zeta}_s$ given by eqn.(8) carries the 3D skyrmion. Therefore, by constructing the desired Hamiltonian in eqn. (6), one can dynamically imprint the 3D skyrmion to a pseudo-spin-1/2 BEC in a harmonic trap, where the spinor wavefunction will take the form $\vec{\psi}(\vec{r}) = \sqrt{\rho(\vec{r})}\vec{\zeta}_s$ and $\rho(\vec{r})$ is the Thomas-Fermi profile. By recognizing $\lambda = \gamma = \alpha r T_0/2\hbar$, $\beta = \theta$, $\eta = \phi$ and using eqn.(5), we find the winding number Q=1, which indicates that the spinor given by eqn.(8) carries a 3D skyrmion with winding number Q = 1 in \mathbb{R}^3 .

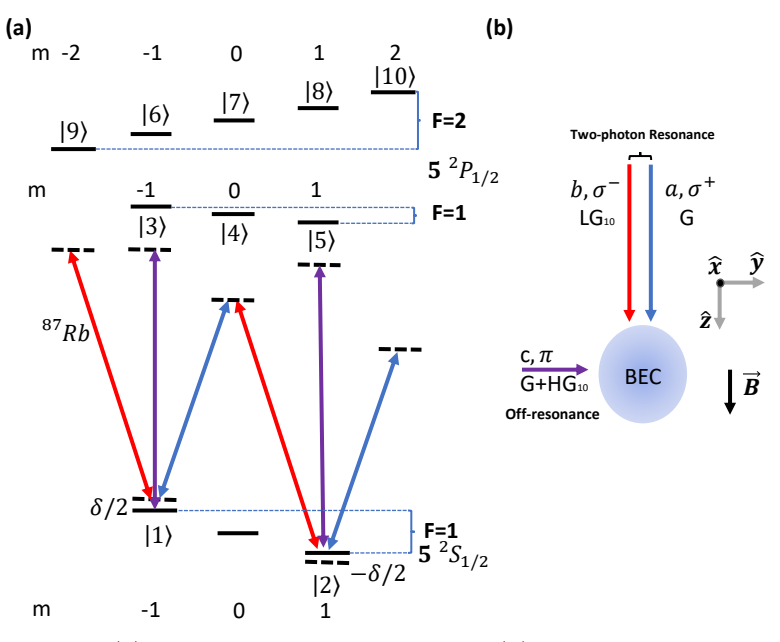


Fig. 1: (a).Level diagram of the system. (b).Laser configurations.

3 Experimental Implementation

Our 3D skyrmion imprinting scheme relies on the Hamiltonian in eqn.(6), which is realized in our experimental protocol by using structured laser beams with different spatial modes.

Generally, the atom-laser interaction can be described by a semi-classical electric dipole interaction Hamiltonian, $H_{dipole} = -\vec{d} \cdot \vec{E}$, where \vec{d} is the dipole moment of the atom and \vec{E} is the electric field. In our calculation we take $^{87}R_b$ BEC as an example, and the pseudo-spin-1/2 states are chosen to be in the F=1 hyperfine ground state manifold of $^{87}R_b$ in a bias magnetic field, \vec{B} . Specifically, $|1\rangle = |5S_{1/2}, F = 1, m_F = -1\rangle$ and $|2\rangle = |5S_{1/2}, F = 1, m_F = 1\rangle$. The other states considered in the Raman process are $|3\rangle = |5P_{1/2}, F = 1, m_F = 1\rangle$, $|6\rangle = |5P_{1/2}, F = 1, m_F = 0\rangle$, $|5\rangle = |5P_{1/2}, F = 1, m_F = 1\rangle$, $|6\rangle = |5P_{1/2}, F = 2, m_F = -1\rangle$, $|7\rangle = |5P_{1/2}, F = 1, m_F = 0\rangle$, $|8\rangle = |5P_{1/2}, F = 2, m_F = 1\rangle$, $|9\rangle = |5P_{1/2}, F = 2, m_F = -2\rangle$ and $|10\rangle = |5P_{1/2}, F = 2, m_F = 2\rangle$. All of the Raman lasers are far detuned from resonance, and the one-photon detunings are much larger than the linewidth of any states that we consider. The energy diagram is shown in Fig.(1).

Starting from H_{dipole} , one can use second-order perturbation theory to construct the effective Hamiltonian of the Raman process [11, 27, 28], and

3D Skyrmion imprinting in a BEC

write down the effective two-level Hamiltonian

$$H_{e} = \frac{1}{2} [\chi_{a0} |\Omega_{a}|^{2} + \chi_{b0} |\Omega_{b}|^{2} + \chi_{c0} |\Omega_{c}|^{2}] \mathbb{1}$$

$$+ \frac{1}{2} \chi_{nd} |\Omega_{a}| |\Omega_{b}| (\cos \phi \sigma_{x} + \sin \phi \sigma_{y})$$

$$+ \frac{1}{2} [\chi_{a} |\Omega_{a}|^{2} + \chi_{b} |\Omega_{b}|^{2} + \chi_{c} |\Omega_{c}|^{2} + \delta] \sigma_{z},$$
(9)

where ϕ is the relative phase between lasers a and b. The coefficients are defined as

$$\chi_{a0} = \frac{C_{1,4}^2}{\Delta_{a1,4}} + \frac{C_{1,7}^2}{\Delta_{a1,7}} + \frac{C_{2,10}^2}{\Delta_{a2,10}},$$

$$\chi_{b0} = \frac{C_{1,9}^2}{\Delta_{b1,9}} + \frac{C_{2,4}^2}{\Delta_{b2,4}} + \frac{C_{2,7}^2}{\Delta_{b2,7}},$$

$$\chi_{c0} = \frac{C_{13}^2}{\Delta_{c1,3}} + \frac{C_{1,6}^2}{\Delta_{c1,6}} + \frac{C_{2,5}^2}{\Delta_{c2,5}} + \frac{C_{2,8}^2}{\Delta_{c2,8}},$$

$$\chi_a = \frac{C_{1,4}^2}{\Delta_{a1,4}} + \frac{C_{1,7}^2}{\Delta_{a1,7}} - \frac{C_{2,10}^2}{\Delta_{a2,10}},$$

$$\chi_b = \frac{C_{1,9}^2}{\Delta_{b1,9}} - \frac{C_{2,4}^2}{\Delta_{b2,4}} - \frac{C_{2,7}^2}{\Delta_{b2,7}},$$

$$\chi_c = \frac{C_{13}^2}{\Delta_{c1,3}} + \frac{C_{1,6}^2}{\Delta_{c1,6}} - \frac{C_{2,5}^2}{\Delta_{c2,5}} - \frac{C_{2,8}^2}{\Delta_{c2,8}},$$

$$\chi_{nd} = (\frac{1}{\Delta_{a1,4}} + \frac{1}{\Delta_{b2,4}})C_{1,4}C_{2,4} + (\frac{1}{\Delta_{a1,7}} + \frac{1}{\Delta_{b2,7}})C_{1,7}C_{2,7},$$

where the Rabi frequencies are given by $\Omega_k = \vec{d}_{D1} \cdot \vec{E}_k/\hbar$, and the one-photon detunings by $\Delta_{ki,j} = \omega_k - (\omega_i - \omega_j)$. In both definitions, k = a, b, c, i = 1, 2 and j = 4, 5, 6, 7, 8, 9, 10. In the definition of Ω_k , \vec{d}_{D1} is the dipole moment for the D₁ transitions of ⁸⁷Rb and $C_{i,j}$ are the Clebsch-Gordon coefficients for specific transitions.

To create the synthetic magnetic monopole field Hamiltonian, we need each the components of σ_x , σ_y and σ_z to be proportional to x,y,z with the same magnitudes. To achieve this, we consider introducing different spatial modes to lasers a, b, c. In our protocol, we consider laser a to be a Gaussian beam along the z-axis, laser b to be a Laguerre-Gaussian beam, LG_{10} , along the z-axis and laser c to be a superposition of a Gaussian beam and a Hermite-Gaussian beam, HG_{01} , of the same frequency along the y-axis. In addition, we consider the size of the atom cloud to be much smaller than the beam waists, w_0 , so that in the regime we consider, $x,y,z \ll w_0$ (wide-beam approximation). In this case, the Rayleigh range of the beams are much larger than the size of the BEC. Therefore, we can regard the Gaussian beam as plane wave, and assume that all of the Gouy phases and quadratic phases of the beams are

negligible. Notice that the 1 component is approximately uniform if we take the wide beam approximation since all of the spatial dependent terms are negligible due to the small ratio $(x^2+y^2)/w_0^2$ and $(x^2+z^2)/w_0^2$. Note that since $x=\rho\cos\phi$ and $y=\rho\sin\phi$, the second term in eqn.(9) is automatically proportional to $x\sigma_x+y\sigma_y$. The exact analytical forms of the laser beams are written as $\Omega_a=\tilde{\Omega}_a exp\{-\frac{\rho^2}{w_0^2}\},~\Omega_b=\tilde{\Omega}_b\frac{\rho}{w_0}exp\{-i\phi\}exp\{-\frac{\rho^2}{w_0^2}\},~\Omega_c^G=\tilde{\Omega}_c^Gexp\{-\frac{x^2+z^2}{w_0^2}\}$ and $\Omega_c^H=\tilde{\Omega}_c^H\frac{z}{w_0}exp\{-\frac{x^2+z^2}{w_0^2}\}$. We define $\tilde{\Omega}_a,~\tilde{\Omega}_b,~\tilde{\Omega}_c^H$, and $\tilde{\Omega}_c^G$ as the spatially independent magnitude of the Rabi frequencies of each beam, where superscripts H and G stand for Hermit-Gaussian and Gaussian beams. Since we take the wide-beam approximation, we can regard $\exp\{-(x^2+y^2)/w_0^2\}$ and $\exp\{-(x^2+z^2)/w_0^2\}$ to be 1. To make the σ_z component proportional to z, we need to make sure that the Rabi frequencies satisfy the following conditions:

$$\tilde{\Omega}_{c}^{G2} + \frac{\chi_{a}\tilde{\Omega}_{a}^{2} + \delta}{\chi_{c}} = 0,
2\chi_{c}\tilde{\Omega}_{c}^{G}\tilde{\Omega}_{c}^{H}\cos\theta_{c} = \chi_{nd}\tilde{\Omega}_{a}\tilde{\Omega}_{b},$$
(11)

where θ_c is the relative phase between the two components of laser c. In the wide-beam approximation, $\frac{\rho}{w_0} \ll 1$ and $\frac{z}{w_0} \ll 1$, and thus we can neglect the spatially dependent AC Stark shift terms in the diagonal matrix elements, namely, $\chi_{a0}\tilde{\Omega}_a^2 + \chi_{c0}\tilde{\Omega}_c^{G^2} \gg \chi_{b0}\tilde{\Omega}_b^2, \chi_{c0}\tilde{\Omega}_c^{H^2}, \chi_{a0}\tilde{\Omega}_a^2 + \chi_{c0}\tilde{\Omega}_c^{G^2} \gg 2\chi_{c0}\tilde{\Omega}_c^G\tilde{\Omega}_c^H\cos\theta_c$ and $2\chi_c\tilde{\Omega}_c^G\tilde{\Omega}_c^H\cos\theta_c \gg \chi_b\tilde{\Omega}_b^2, \chi_c\tilde{\Omega}_c^{H^2}$. From the above conditions and eqn.(11) we get

$$\tilde{\Omega}_{c}^{G} = \sqrt{-\frac{\chi_{a}\tilde{\Omega}_{a}^{2} + \delta}{\chi_{c}}},
\tilde{\Omega}_{c}^{H} = \frac{\chi_{nd}\tilde{\Omega}_{a}\tilde{\Omega}_{b}}{2\cos\theta_{c}\sqrt{-\chi_{c}(\chi_{a}\tilde{\Omega}_{a}^{2} + \delta)}}.$$
(12)

When all these conditions are satisfied the effective Hamiltonian can be well approximated by

$$H_e(\vec{r}) \approx \hbar \alpha (x\sigma_x + y\sigma_y + z\sigma_z),$$
 (13)

where we ignored the 1 term as it only introduced a global phase to the system under the wide-beam limit and can not be measured.

In addition, it is worthwhile to mention the case of an asymmetric harmonic trap with trapping frequencies $(\omega_{\perp}, \omega_{\perp}, \omega_z)$, where ω_{\perp} and ω_z are the trapping frequency along the radial and longitudinal directions, respectively, and the BEC in the trap is no longer spherically symmetric. One can overcome such a problem by transforming into a rescaled coordinates defined by $(x', y', z') = (\frac{w_{\perp}}{w_0} x, \frac{w_{\perp}}{w_0} y, \frac{w_z}{w_0} z)$, then the trap becomes spherically symmetric in this stretched (rescaled) coordinate system and the mathematical formalism stays the same as the case in a spherically symmetric

harmonic trap. This can be achieved by adjusting the Raman field amplitudes Ω_b and Ω_c^H to match the aspect ratio of the trap, so that they take the form $\Omega_b = \tilde{\Omega}_b' \frac{\rho}{w_\perp} exp\{-i\phi\} exp\{-\frac{\rho^2}{w_0^2}\}$ and $\Omega_c^H = \tilde{\Omega}_c^{H,'} \frac{z}{w_z} exp\{-\frac{x^2+z^2}{w_0^2}\}$, where $\tilde{\Omega}_b' = \tilde{\Omega}_b w_\perp/w_0$ and $\tilde{\Omega}_c^{H,'} = \tilde{\Omega}_c^H w_z/w_0$, respectively.

To implement the laser field c, we can separate two of the beams transmitted through an acousto-optical modulator (AOM), and keep one as a Gaussian beam, and then use a digital-micromirror device(DMD), spatial light modulator (SLM) or other methods to produce a Hermite-Gaussian beam from the second. We can then merge the two beams to get laser c. For our example in section.4, we can calculate the Rabi frequencies to be $\tilde{\Omega_a} \approx 271.17 \text{kHz}$, $\tilde{\Omega_b} \approx 27.12 \text{kHz}$, $\tilde{\Omega_c}^G \approx 557.67 \text{kHz}$ and $\tilde{\Omega_c}^H \approx 26.15 \text{kHz}$. The corresponding bias magnetic field is B=10G and the two-photon detuning $\delta=0$. The laser frequencies considered in our calculations are $\omega_a=\omega_L-2\pi\times440 \text{MHz}$ with σ^+ polarization, $\omega_b=\omega_L-2\pi\times454 \text{MHz}$ with σ^- polarization and $\omega_c=\omega_L+2\pi\times400 \text{MHz}$ with π polarization, where ω_L is the angular frequency corresponding to the ^{87}Rb D_1 transition, as shown in Fig.1. All of the parameters considered in our calculations can be easily achieved in the lab.

4 Numerical simulations

For a single particle, one can apply the evolution operator in eqn. (7) to the spinor state $\vec{\xi_0}$, and in theory the 3D skyrmion will be imprinted to the spinor wavefunction after certain time T_0 . However, there exists a non-linear interaction for a BEC in a dipole trap, which may affect the imprinting process. Therefore, it is necessary to examine the dynamical imprinting scheme of the 3D skyrmion with the non-linear interaction taken into account. In the mean-field limit, the BEC wavefunction, $\vec{\psi}$, satisfies a Gross-Pitaevskii (GP) equation

$$i\hbar \frac{\partial \vec{\psi}(\vec{r},t)}{\partial t} = \left(\frac{p^2}{2M} + V_{trap} + H_e(\vec{r}) + H_{int}\right) \vec{\psi}(\vec{r},t),\tag{14}$$

where $V_{trap} = \frac{1}{2}M\omega_0^2r^2$ is the trapping potential, $H_{int} = \int (c_0S_0^2 + c_2S_3^2)dr^3$ is the nonlinear interaction potential between particles with $S_0 = |\vec{\psi}(\vec{r})|^2$, and $S_3 = \vec{\psi}^{\dagger}\sigma_3\vec{\psi}$ and M is the atomic mass.

With the GP equation, we next turn to numerical simulation to examine the effectiveness of our 3D skyrmion imprinting scheme. By applying a finite-element discrete variable representation method [29] and real time propagation with a fourth-order Runge-Kutta method, we perform a numerical simulation of eqn.(14). The pulse duration is $T_0 = 2\hbar\pi/\alpha R_0 \approx 40\mu s$, $\alpha R_0 = 250\omega_0$, $c_0 = 6.72 \times 10^3 \hbar \omega_0 r_0^3$ and $c_1 = -0.005c_0$. $R_0 \approx 6r_0$ is the Thomas-Fermi radius of the BEC cloud with $N = 10^5$ atoms confined in the trapping potential V_{trap} at zero temperature, $\omega_0 = 2\pi \times 100 \text{Hz}$, $t_0 = 2\pi \omega_0^{-1}$ and $r_0 = \sqrt{\hbar/M\omega_0} \approx 1\mu m$ are the trap units for ^{87}Rb .

The numerical simulation versus theoretical calculation results from eqn.(8) are shown in Fig.2. In Fig.2 (a) and (b), we show the population density of

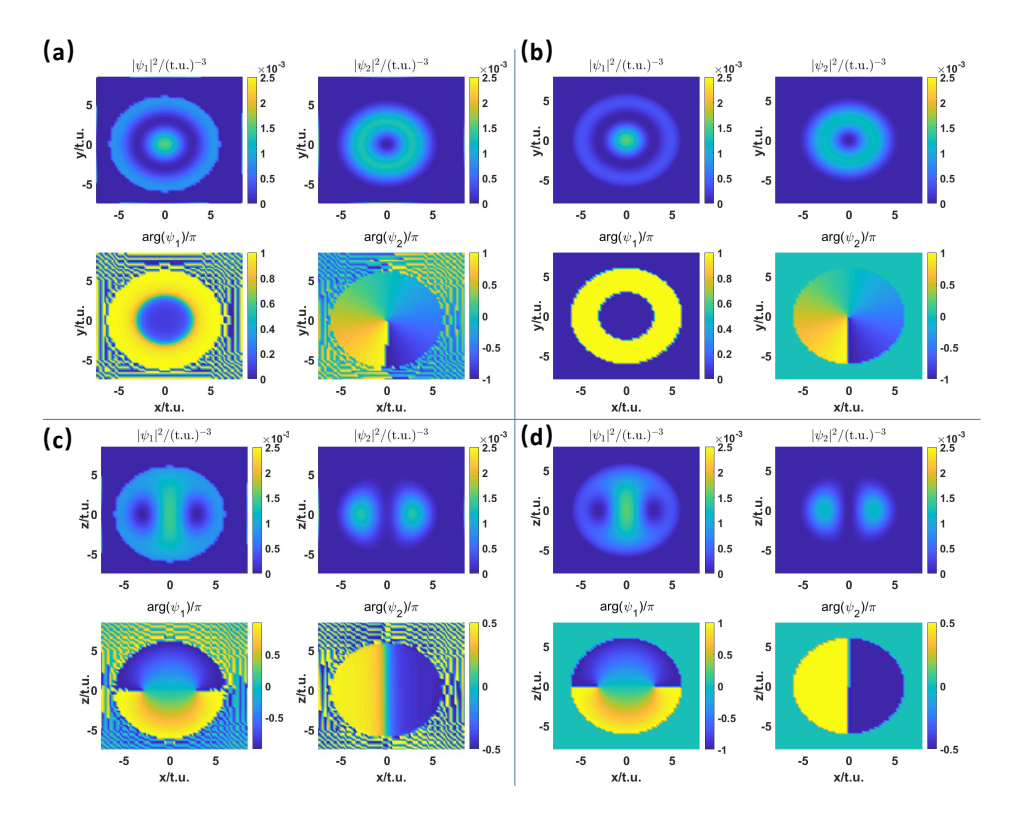


Fig. 2: Population density and phase factor on state $|1\rangle$ and $|2\rangle$ in z=0 plane ((a) numerical results, (b) theoretical results) and in y=0 plane ((c) numerical results, (d) theoretical results). The good agreement between theoretical calculation and GP equation simulation indicates the effectiveness of the imprinting scheme of the 3D skyrmion. t.u. indicates trap units.

each state, $|\psi_1(x,y,0)|^2$ and $|\psi_2(x,y,0)|^2$, in z=0 plane, as well as the phase factor of each component. In Fig.2 (c) and (d), we show the population density of each state $|\psi_1(x,0,z)|^2$ and $|\psi_2(x,0,z)|^2$, in y=0 plane and the phase factor of each component. The figures show a good agreement between the numerical simulation results and the theoretical calculations along with the desired spin texture, such as the vortex ring on $|2\rangle$ component indicated by eqn.(8). Thus, by allowing the BEC to evolve in time from the initial state $(1,0)^T$ in a 3D monopole synthetic magnetic field, one can imprint a three-dimensional skyrmion on a pseudo-spin-1/2 BEC even with the non-linear interaction of the BEC taken into consideration.

5 Observation

For a pseudo-spin-1/2 spinor, one can identify the spatially dependent spinor state by measuring the Stokes parameters (or Bloch vectors). For any spinor $\vec{\xi} = (\xi_1, \xi_2)^T$, the Stokes parameters can be defined as

$$s_{1} = \xi_{1}^{*}\xi_{2} + \xi_{1}\xi_{2}^{*}$$

$$s_{2} = -i(\xi_{1}^{*}\xi_{2} - \xi_{1}\xi_{2}^{*})$$

$$s_{3} = |\xi_{1}|^{2} - |\xi_{2}|^{2},$$
(15)

which satisfy $|s_1|^2 + |s_2|^2 + |s_3|^2 = 1$. If we construct the spinor in eqn.(3), then we can write the Stokes parameters using the coordinates on S^3 , and the vector field formed by the Stokes parameters in \mathbb{R}^3 will become a map from S^3 to \mathbb{R}^3 . Therefore, by measuring the spatially varying map of Stokes parameters, one can reconstruct the 3D skyrmion imprinted in the spinor wavefunction.

To measure the Stokes parameters in our experimental protocol, one can turn off the bias magnetic field, release the BEC from the optical dipole trap, and let the condensate expand during free fall. One can then take a Stern-Gerlach time-of-flight (TOF) image of the ultra cold atom cloud [6, 8, 9, 12, 13, 17, 28] to obtain separated absorption images of the two spin components. By imaging along the y and z-axis, one gets the projections of the spinor population densities to each direction, which can be used to calculate the Stokes parameters of the spinor gas. To measure different Stokes parameters, one can apply a spin rotation after the imprinting process, which can be achieved in many ways such as with radio-frequency [30] or Raman pulses [14]. Using the Stern-Gerlach TOF imaging along different directions, one can identify the topological structure in the BEC cloud and find it is consistent with theoretical calculations.

6 Conclusion and discussion

In this work, we proposed an experimental protocol for imprinting a three-dimensional skyrmion in a ultracold Bose-Einstein condensate via a Raman process with structured laser beams. Our protocol is based on the demonstrated vortex and two-dimensional skyrmion imprinting techniques, and so it is straightforward to implement in the laboratory. By comparing our calculations to a numerical mean-field Gross-Pitaevskii equation simulation, we examined the effectiveness of our imprinting protocol. Also, the imprinting Raman pulse is short enough to avoid the influence of the nonlinear interaction in the BEC, as is verified by our numerical calculation.

Although we only discussed the imprinting scheme of 3D skyrmion with topological charge Q=1, one can extend our method to imprint 3D skyrmions with higher topological charge (e.g. Q=2). This could be done by changing the effective two-level coupling Hamiltonian, H_e , from the form of a monopole-like synthetic magnetic field to a multipole-like synthetic magnetic field [31].

3D Skyrmion imprinting in a BEC

Similar to the monopole case, a multipole-like field could be realized by the superposition of structured optical fields. Our protocol also works for fermionic systems as long as the laser frequencies and detunings are chosen properly.

11

Acknowledgments. We thank Elisha Haber for discussion. Zekai Chen and Nicholas P. Bigelow are supported by NSF grant PHY 1708008 and NASA/JPL RSA 1656126. S.X. Hu is supported by the Department of Energy National Nuclear Security Administration under Award Number DE-NA0003856, the University of Rochester, and the New York State Energy Research and Development Authority. The support of DOE does not constitute an endorsement by DOE of the views expressed in this paper. The authors thank the Center for Integrated Research Computing (CIRC) at the University of Rochester for providing computational resources and technical support.

References

- [1] Shankar, R.. Applications of topology to the study of ordered systems. Journal de Physique, 38(11), 1405-1412 (1977).
- [2] Volovik, G. E., Mineev, V. P.. Particle-like solitons in superfluid ³He phases. Zh. Eksp. Teor. Fiz, 73, 767-773 (1977).
- [3] Anderson, P. W. and Toulouse, G.. Phase slippage without vortex cores: vortex textures in superfluid He 3. Physical Review Letters, 38(9), 508 (1977).
- [4] Mermin, N. D. and Ho, T. L.. Circulation and angular momentum in the a phase of superfluid Helium-3. Physical Review Letters, 36(11), 594 (1976).
- [5] Matthews, M. R., Anderson, B. P., Haljan, P. C., Hall, D. S., Wieman, C. E., Cornell, E. A.. Vortices in a Bose-Einstein condensate, Physical Review Letters 83 (13), 2498 (1999).
- [6] Ray, M. W., Ruokokoski, E., Tiurev, K., Möttönen, M., Hall, D. S.. Observation of Dirac monopoles in a synthetic magnetic field. Observation of Dirac monopoles in a synthetic magnetic field, Nature 505 (7485), 657-660 (2014).
- [7] Ray, M. W., Ruokokoski, E., Tiurev, K., Möttönen, M., Hall, D. S.. Observation of isolated monopoles in a quantum field, Science 348 (6234), 544-547 (2015).
- [8] Hall, D. S., Ray, M. W., Tiurev, K., Ruokokoski, E., Gheorghe, A. H., Möttönen, M.. Tying quantum knots, Nature Physics 12 (5), 478-483 (2016).
- [9] Lee, W., Gheorghe, A. H., Tiurev, K., Ollikainen, T., Möttönen, M., Hall, D. S.. Synthetic electromagnetic knot in a three-dimensional skyrmion, Science advances 4 (3), eaao3820 (2018).
- [10] Choi, J. Y., Kang, S., Seo, S. W., Kwon, W. J., Shin, Y. I.. Observation of a geometric Hall effect in a spinor Bose-Einstein condensate with a skyrmion spin texture. Physical Review Letters, 111(24), 245301 (2013).

- [11] Wright, K. C., Leslie, L. S., Bigelow, N. P.. Optical control of the internal and external angular momentum of a Bose-Einstein condensate, Physical Review A, 77 (4), 041601 (2008).
- [12] Wright, K. C., Leslie, L. S., Hansen, A., Bigelow, N. P.. Sculpting the vortex state of a spinor BEC, Physical Review Letters, 102 (3), 030405 (2009).
- [13] Leslie, L. S., Hansen, A., Wright, K. C., Deutsch, B. M., Bigelow, N. P.. Creation and detection of skyrmions in a Bose-Einstein condensate, Physical Review Letters, 103 (25), 250401 (2009).
- [14] Schultz, J. T., Hansen, A., and Bigelow, N. P., A Raman Waveplate for Spinor Bose-Einstein condensates, Optics Letters 39, 4271-4273 (2014).
- [15] Schultz, J. T., Hansen, A., J. D. Murphree, M. Jayaseelan, and Bigelow, N. P., Creating full-Bloch Bose-Einstein condensates with Raman q-plates, Journal of Optics 18(6), 64009 (2016).
- [16] Schultz, J. T., Hansen, A., J. D. Murphree, M. Jayaseelan, and Bigelow, N. P., Raman fingerprints on the Bloch sphere of a spinor Bose-Einstein condensate, Journal of Modern Optics 63 (2016).
- [17] Hansen, A., Schultz, J. T., and Bigelow, N. P., Singular atom optics with spinor Bose-Einstein condensates, Optica 3(4) 355-361 (2016).
- [18] Rubinsztein-Dunlop, H., Forbes, A., Berry, M. V., Dennis, M. R., Andrews, D. L., Mansuripur, M., ... Weiner, A. M.. Roadmap on structured light. Journal of Optics, 19(1), 013001 (2016).
- [19] Wright, D. C. and Mermin, N. D.. Crystalline liquids: the blue phases. Reviews of Modern physics, 61(2), 385 (1989).
- [20] Kevrekidis, P. G., Carretero-González, R., Frantzeskakis, D. J., Malomed, B. A. and Diakonos, F. K.. Skyrmion-like states in two-and three-dimensional dynamical lattices. Physical Review E, 75(2), 026603 (2007).
- [21] Morinari, T.. Half-skyrmion picture of a single-hole-doped CuO 2 plane. Physical Review B, 72(10), 104502 (2005).
- [22] Pereira, A. R., Ercolessi, E. and Pires, A. S. T.. Pseudo-particles picture in single-hole-doped two-dimensional Néel ordered antiferromagnet. Journal of Physics: Condensed Matter, 19(15), 156203 (2007).
- [23] Ruostekoski, J., Anglin, J. R.. Creating vortex rings and threedimensional skyrmions in Bose-Einstein condensates, Physical Review

- 3D Skyrmion imprinting in a BEC
- Letters, 86 (18), 3934 (2001).
- [24] Kawaguchi, Y., Ueda, M., Spinor bose–einstein condensates, Physics Reports, 520 (5), 253-381 (2012).
- [25] Al Khawaja, U., Stoof, H.. Skyrmions in a ferromagnetic Bose–Einstein condensate. Nature, 411(6840), 918-920 (2001).
- [26] Al Khawaja, U., Stoof, H. T. C.. Skyrmion physics in Bose-Einstein ferromagnets. Physical Review A, 64(4), 043612 (2001).
- [27] Cohen-Tannoudji, C., Dupont-Roc, J., Grynberg, G.. Atom-photon interactions: basic processes and applications, pp. 678. ISBN 0-471-29336-9. Wiley-VCH, (1998).
- [28] Chen, Z., Murphree, J. D., Bigelow, N. P., SU(2) geometric phase induced by a periodically driven Raman process in an ultracold dilute Bose gas, Physical Review A 101 (1), 013606 (2020).
- [29] Schneider, B. I., Collins, L. A., Hu, S. X.. Parallel solver for the time-dependent linear and nonlinear Schrödinger equation, Physical Review E, 73 (3), 036708 (2006).
- [30] Sugawa, S., Salces-Carcoba, F., Perry, A. R., Yue, Y., Spielman, I. B.. Second Chern number of a quantum-simulated non-Abelian Yang monopole. Science, 360(6396), 1429-1434 (2018).
- [31] Luo, H. B., Li, L., Liu, W. M., three-Dimensional Skyrmions with Arbitrary topological number in a Ferromagnetic Spin-1 Bose-einstein condensate. Scientific reports, 9(1), 1-10 (2019).